IOP Publishing Nanotechnology
Nanotechnology 28 (2017) 425204 (8pp) https://doi.org/10.1088/1361-6528/aa82d7

Realization of wide circadian variability by quantum dots-luminescent mesoporous silica-based white light-emitting diodes

Bin Xie[1,2], Jingjing Zhang[1,3], Wei Chen[2], Junjie Hao[2], Yanhua Cheng[1], Run Hu[1], Dan Wu[4], Kai Wang[2,5] and Xiaobing Luo[1,5]

[1] School of Energy and Power Engineering, Huazhong University of Science and Technology, Wuhan, 430074, People's Republic of China
[2] Department of Electrical & Electronic Engineering, Southern University of Science and Technology, Shenzhen, 518055, People's Republic of China
[3] School of Automation, China University of Geosciences, Wuhan, 430074, People's Republic of China
[4] School of Electrical & Electronic Engineering, Nanyang Technological University, Singapore, 639798, Singapore

E-mail: wangk@sustc.edu.cn and luoxb@hust.edu.cn

Received 24 May 2017, revised 20 July 2017
Accepted for publication 28 July 2017
Published 25 September 2017

Abstract

Human comfort has become one of the most important criteria in modern lighting architecture. Here, we proposed a tuning strategy to enhance the non-image forming photobiological effect on the human circadian rhythm based on quantum-dots-converted white light-emitting diodes (QDs-WLEDs). We introduced the limiting variability of the circadian action factor (CAF), defined as the ratio of circadian efficiency and luminous efficiency of radiation. The CAF was deeply discussed and was found to be a function of constraining the color rendering index (CRI) and correlated color temperatures. The maximum CAF variability of QDs-WLEDs was found to be dependent on the QDs' peak wavelength and full width at half maximum. With the optimized parameters, the packaging materials were synthesized and WLEDs were packaged. Experimental results show that at CRI $>$ 90, the maximum CAF variability can be tuned by 3.83 times (from 0.251 at 2700 K to 0.961 at 6500 K), which implies that our approach could reduce the number of tunable channels, and could achieve wider CAF variability.

Keywords: quantum dots, light-emitting diodes, optical effects on vision, optical design

(Some figures may appear in colour only in the online journal)

1. Introduction

Nowadays, the requirements of indoor lighting are becoming more and more rigorous. People are no longer satisfied with lighting with high brightness, high efficiency and high uniformity. On the contrary, the concept of humanistic lighting is frequently mentioned and discussed, which means taking human comfort into consideration when designing or choosing proper lighting products. On the other hand, white light-emitting diodes (WLEDs) have triggered the evolution of modern lighting and lifestyle with the penetration and replacement of traditional light sources [1–3]. However, the most widely-used WLEDs are based on blue-light-rich chips with yellow-, red-, and green-phosphors [4, 5]. Due to the rich blue light, objects look unrealistic and it is harmful to our eyes over the years. Moreover, blue light can affect human circadian physiology, alertness and cognitive performance levels through the excitation of the intrinsically photosensitive retinal ganglion cells containing melanopsin photopigment [6, 7]. Such photobiologically efficacious light might be desired in the morning hours and during the day, but should be avoided in the late evening hours and during the night to prevent unwanted disruption of the human circadian rhythm [8–11]. Therefore, artificial lighting sources with high

[5] Authors to whom any correspondence should be addressed.

color rendering index (CRI) performance as well as dynamic circadian action, which relies on the time-of-day dependent modulation of lighting conditions, is in urgent need for indoor conditions [12–14].

One feasible way to relieve this problem is to tune the light spectrum in terms of the full width at half maximum (FWHM), wavelength and intensity of R, G, and B components of the light source. Quantum dots (QDs), due to their unique optical characteristics such as narrow emission spectra, tunable emission wavelength, and high quantum yields, are quite appealing as the proper candidates for tuning the light spectrum. It was reported that QDs-integrated WLEDs can realize excellent CRI characteristics (Ra and R9 up to 95) and remarkable high luminous efficiency (LE) [15–17]. However, there are few works referring to the circadian tuning of QDs-WLEDs, and their limiting circadian variability has not been revealed.

Here, we developed a spectra model with a blue LED chip, yellow-emissive phosphor and red-emissive QDs-luminescent mesoporous silica (QDs-LMS). Based on the spectra model, we could achieve wide circadian variability as well as excellent color rendering ability. Spectral optimization was performed to investigate the limits of circadian variability as a function of QDs' peak wavelength and FWHM. Subsequently, WLEDs with optimized QD configuration were fabricated to validate the optimization.

2. Model and experiments

2.1. Spectral model setup

The circadian action factor (CAF) a_c, which is defined as the ratio of the circadian efficacy to luminous efficacy, is obtained as [18]:

$$a_c = \mathrm{K}\int_{380}^{780} C(\lambda)P(\lambda)d\lambda \Big/ \int_{380}^{780} V(\lambda)P(\lambda)d\lambda. \qquad (1)$$

Where $C(\lambda)$ is the circadian spectral efficiency function which peaks at about 464 nm using Gall's model [18], $P(\lambda)$ is the spectral power distribution (SPD) of the light source, $V(\lambda)$ is the photopic eye-sensitivity function, and K is a normalization constant which makes $a_c = 1$ for the SPD of the CIE standard illuminant D_{65}.

The CAF of the QDs-WLEDs can be dynamically tuned by varying the partial radiant fluxes and peak wavelength of the three components. To find the optimal configuration for maximum circadian action variability, an objective function F, which is the ratio of the highest and lowest values of CAF, is to be maximized:

$$F(\lambda_{1i};\ \lambda_{2i};\ p_{1i};\ p_{2i})_{i=1,2,3} = \frac{a_{c,\max}(\lambda_{11},\ \lambda_{12},\ \lambda_{13};\ p_{11},\ p_{12},\ p_{13})}{a_{c,\min}(\lambda_{21},\ \lambda_{22},\ \lambda_{23};\ p_{21},\ p_{22},\ p_{23})} \qquad (2)$$

where p_{1i} and λ_{1i} ($i = 1$, 2 and 3) are the peak wavelengths and relative partial radiant fluxes of the spectral components for the highest CAF, and p_{2i} and λ_{2i} are those for the lowest CAF, respectively. The objective function is also subjected to additive color mixing constraints such as the minimal values of the LER and CRI. In the optimization process, we restricted the three spectral components to those having Gaussian line shapes with FWHM of 30 nm, 103 nm and 32 nm, respectively. The optimization problem is a nonlinear programming problem; therefore, we adopted a genetic algorithm with penalty functions to obtain the optimal results [19, 20]. The penalty functions will force the solution of the equation to approach the feasible solution that meets the constraints. We searched the regions of $\lambda_{11} = \lambda_{21} = 455$ nm, 500 nm $\leqslant (\lambda_{12},\ \lambda_{22}) \leqslant$ 600 nm, and 600 nm $\leqslant (\lambda_{13},\ \lambda_{23}) \leqslant$ 750 nm, and a series of solutions were obtained for the QDs-WLEDs having constant CCTs from 2700–6500 K, with an interval of 60 K.

2.2. Preparation of QDs-LMS

The red-emissive CdSe/ZnS core/shell QDs were prepared by the Tri-n-Octylphosphine (TOP)-assisted successive ionic layer adsorption and reaction (SILAR) method [17, 21]. This synthesis route breaks through the bottleneck of low quantum yields of QDs at high coverage of the shell. To fabricate the QDs-WLEDs, QDs have to be mixed with phosphor and thermal-curable silicone gel, and then integrated with a blue LED chip to achieve high CRI and wide circadian variability [22–25]. However, due to the toxicity of QDs' surface ligands (for example, trioctyl phosphine oxide, TOPO) to the Pt catalyst (chloroplatinic acid basis) of silicone, QDs cannot be directly mixed with silicone gel. To solve this problem, we incorporated the QDs into mesoporous silica microspheres via a swelling and evaporation method, to form the QDs-luminescent mesoporous silica (QDs-LMS).

Figure 1 illustrates the schematic of this method. Briefly, 200 μl QDs solution (containing 10 mg QDs), 1 g MS and 30 ml n-hexane was placed into a 100 ml single-necked flask, then degassed under vacuum at 60 °C for 10 min with magnetic stirring, and then purged with argon (Ar) to eliminate any air. The mixture was maintained at 60 °C for swelling and solvent evaporation under stirring at 1000 rpm min^{-1} for about 2 h. During this process, the mesoporous structure allowed the QDs to enter into the MS, and further evaporation drove the QDs deeper into the pores. The obtained QDs-LMS were precipitated after 30 min of standing, and then washed twice with an excess of *n*-hexane to remove the QDs absorbed on the MS surface. The final QDs-LMS were obtained after a further drying process in vacuum oven at 50 °C under nitrogen protection.

2.3. Fabrication of QDs-WLEDs

A blue InGaN LED chip with peak wavelength of 455 nm and FWHM of 30 nm, and yellow-greenish-emissive YAG: Ce phosphor with peak wavelength of 550 nm and FWHM of 103 nm were used as purchased without any treatment. Typically, 0.1 g of phosphor, 0.3 g of QDs-LMS and 1 g silicone gel (Dow corning OE6550) were mixed, then the mixture was stirred for 20 min to be dispersed uniformly. Bubbles introduced during the stirring process were removed

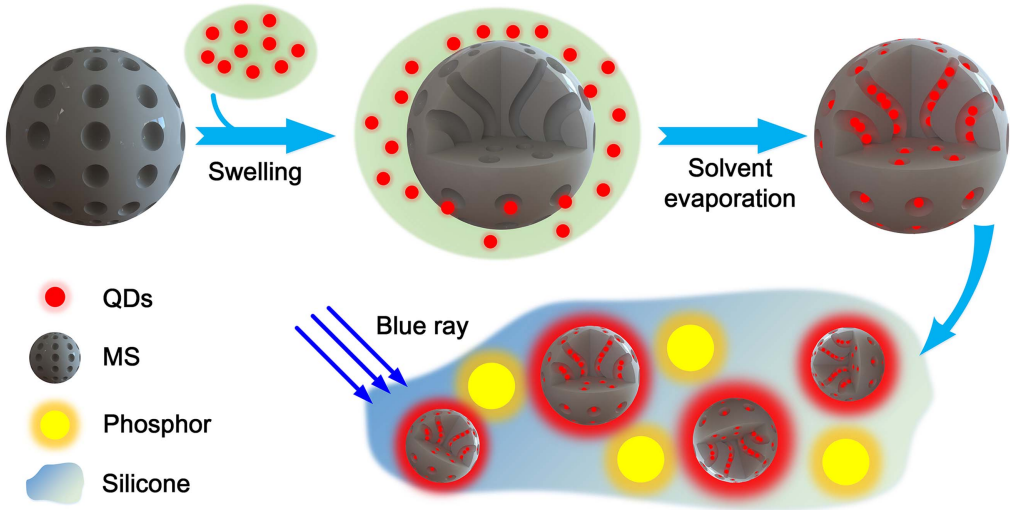

Figure 1. Schematic showing the preparation of QDs-LMS by the swelling and evaporation method.

by applying alternating cycles of vacuum. QDs-WLEDs were fabricated by coating the QDs-LMS/phosphor silicone gel onto the LED chip. Finally the QDs-WLEDs were placed in the vacuum oven at 150 °C and kept there for 1 h. Note that the optical performance of the as-prepared QDs-WLEDs can be tuned by changing the relative proportion of QDs-LMS and phosphor, and the coating volume of QDs-LMS/phosphor silicone gel.

3. Results and discussion

3.1. Spectral optimization of QDs-WLEDs

Figure 2 shows the dependences of the maximum/minimum attainable CAF values and the maximized circadian variability as a function of CCT (Pareto frontiers) at different CRI limitations of CRI > 75, CRI > 90 and CRI > 95. Compared to the 2700 K black-body radiator and common warm-white pc-LED, which have a CAF of 0.363 and about 0.3, respectively, it is found that our approach could have both higher and lower circadian actions. Take CRI >75 for example; the CAF of 2700 K QDs-WLEDs could vary from 64–124% (0.233–0.449) of the CAF values of the incandescent spectrum with the same color temperature. This indicates that warm-white QDs-WLEDs could introduce less melatonin suppression effect compared to that of an incandescent lamp. At CRI > 90, the CAF value can be tuned by 3.83 times (from 0.251 at 2700 K to 0.961 at 6500 K). As a comparison, a theoretical CAF variability of 3.11 times (ranging from 0.351–1.038) can be achieved at a color fidelity index of 90, based on four channels of LED chips spectral optimization [26]. Based on three-channel tunable LED cluster spectral optimization, the theoretical CAF can be tuned by 3.25 times (ranging from 0.294–0.957) while maintaining a CRI of 90 [27]. Therefore, our QDs-WLEDs can reduce the number of tunable channels and achieve wider CAF variability.

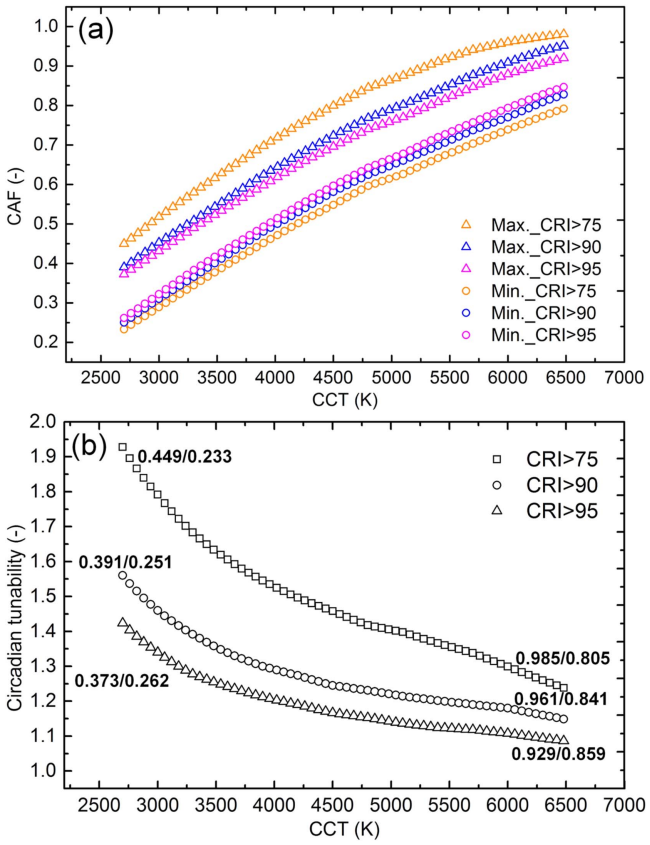

Figure 2. (a) Maximum and minimum achievable CAF values as functions of CCT, with CRI limitation of 75, 90 and 95. (b) The corresponding circadian variability as a function of CCT.

It is seen from figure 2(b) that there is a trade-off between maximal circadian variability and CRI. This is attributed to the decrease of maximum CAF and the increase of minimum CAF with increasing CRI at a certain color temperature, which narrows the tunable range of WLEDs spectra. For instance, at CCT = 2700 K and CRI > 75, the maximum and minimum CAF is 0.449 at peak wavelength of λ_{12} = 523 nm,

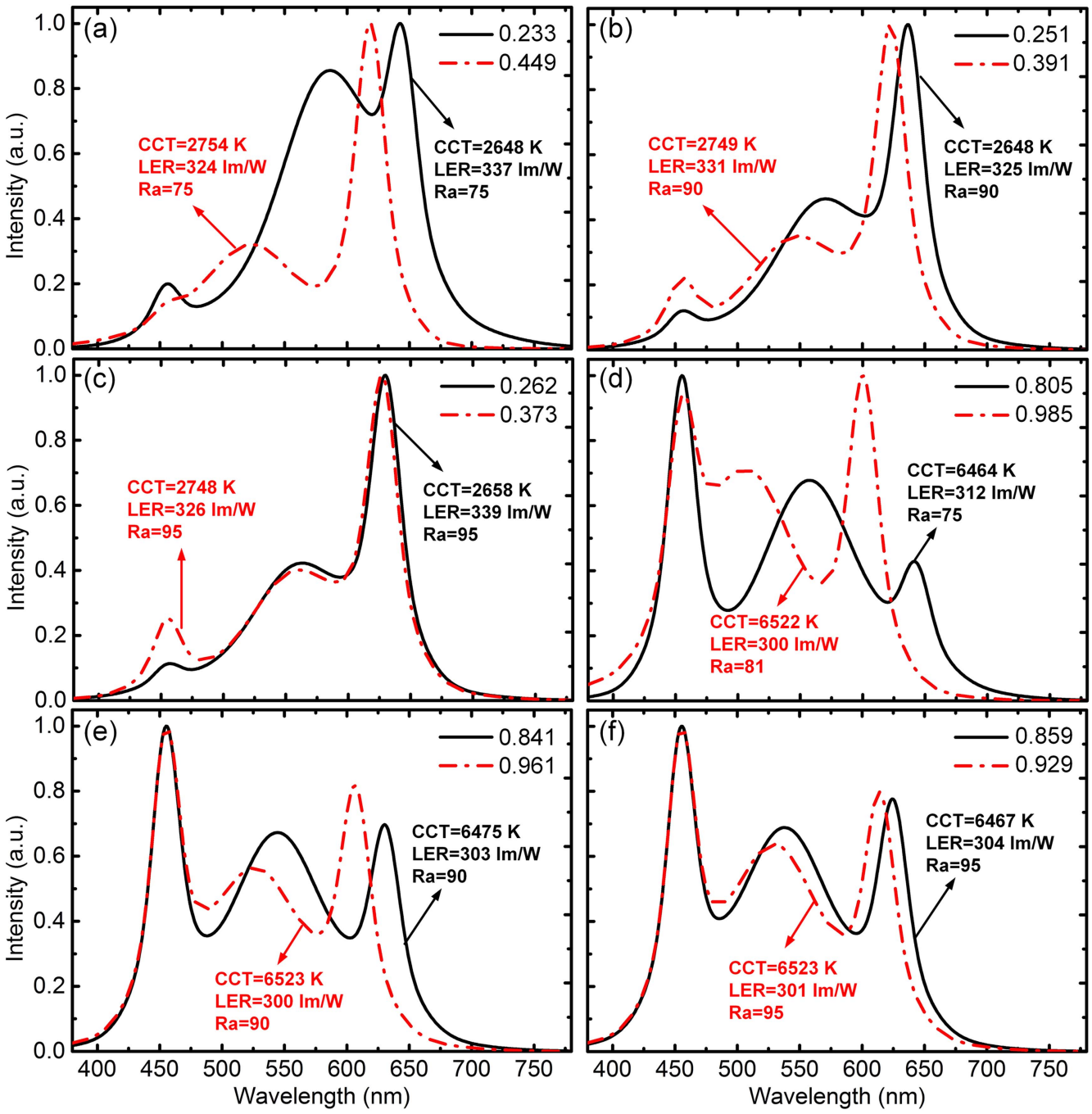

Figure 3. The corresponding spectra of maximum and minimum achievable CAF values as function of CCT, with CRI limitation of 75, 90 and 95.

$\lambda_{13} = 619$ nm, and 0.233 at peak wavelength of $\lambda_{22} = 585$ nm, $\lambda_{23} = 644$ nm, respectively, resulting in a circadian variability of 1.93. By increasing CRI limitation to 90, the maximal circadian variability is reduced to 1.58 ($a_{c,\min} = 0.251$ and $a_{c,\max} = 0.391$) at peak wavelengths of 548 nm, 623 nm, 569 nm, and 637 nm. Alternatively, by increasing CRI limitation to 95, the maximal circadian variability is reduced to 1.42 ($a_{c,\min} = 0.262$ and $a_{c,\max} = 0.373$) at peak wavelengths of 559 nm, 627 nm, 561 nm, and 630 nm. Note that although the increase of CCT reduces the circadian variability significantly, it has a small effect on reducing the tunable range of CAF. The decrease of circadian variability is mainly due to the increase of minimum CAF. Figure 3 shows the corresponding spectra of maximum and minimum achievable CAF values as function of CCT, with CRI limitations of 75, 90 and 95.

Figure 4(a) depicts the dependence of the maximized circadian variability, which is defined as the ratio of the maximum CAF at CCT = 6500 K to the minimum CAF at CCT = 2700 K, on QDs peak wavelength at a constraint of CRI > 80. The QDs peak wavelength varies from 610–670 nm, which can be achieved by tuning the molar ratio

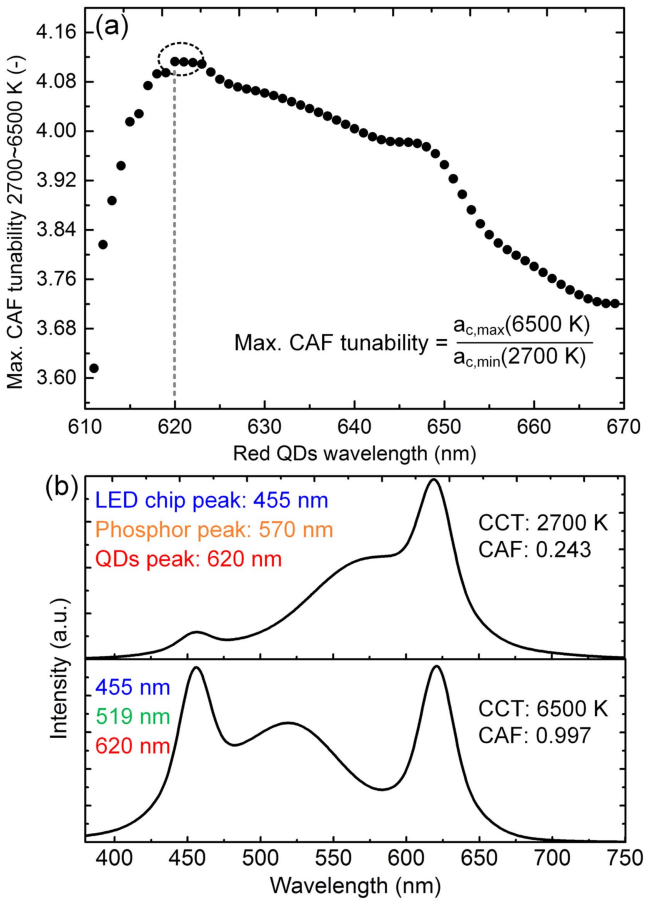

Figure 4. (a) Dependence of the maximized circadian variability on QDs peak wavelength. (b) The optimized spectra for minimum (upper) and maximum (down) CAF.

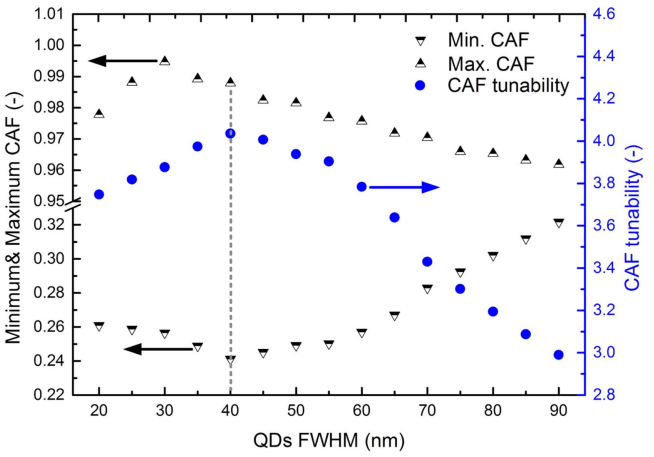

Figure 5. Maximum and minimum CAF and circadian variability as a function of the QDs FWHM, which varies from 20–90 nm with an interval of 5 nm.

of core and shell precursors during the synthesis process. For instance, the PL emission wavelength of InP/ZnS core/shell QDs can be continuously tuned from the blue to the near-infrared region by increasing the ratio of InP precursors to zinc stearate from 1:2 to 16:1 [28].

While varying the QDs peak wavelength from 610–670 nm, the maximized circadian variability increases at first and goes down later after reaching its maximum value of 4.11 at QDs peak wavelength of 620 nm. The minimum CAF = 0.243 is achieved at CCT = 2700 K with a peak wavelength of 455 nm, 570 nm, and 620 nm, and the maximum CAF = 0.997 is obtained at CCT = 6500 K with peak wavelengths of 455 nm, 519 nm, and 620 nm. The optimized spectra are displayed in figure 4(b). One finds that compared to the results in figure 2, the QDs peak wavelength of 620 nm can result in the maximum CAF but not the minimum CAF. Therefore, the optimized QDs peak wavelength of 620 nm for maximized circadian variability is a compromise between the maximum and minimum achievable CAF.

To further investigate the function of QDs FWHM on the maximized circadian variability of QDs-WLEDs, a series of optimization was performed by changing QDs FWHM from 20–90 nm, with an interval of 5 nm. The FWHM can be tuned by varying the size distribution during the reaction process. For instance, FWHM from 20–40 nm can be realized by core–shell chalcogenide-based QDs such as CdSe/CdS due to the narrow size distributions of the luminescent CdSe cores, combined with an epitaxially grown, electronically passivating CdS shell [29]. FWHM from 40–90 nm can be achieved by tuning the concentration of the shell precursor source while keeping the other precursor concentration constant [30].

This objective is to obtain the minimum attainable CAF at CCT = 2700 K with constraints of $\lambda_{11} = 455$ nm, $\lambda_{12} = 570$ nm, $\lambda_{13} = 620$ nm, and CRI > 80, and to obtain the maximum CAF at CCT = 6500 K with constraints of $\lambda_{21} = 455$ nm, $\lambda_{22} = 519$ nm, $\lambda_{23} = 620$ nm, and CRI > 80. Therefore, the optimization process searches the optimal QDs FWHM for maximized circadian variability based on the optimal results of QDs peak wavelength. Figure 5 displays the dependence of maximum/minimum CAF and circadian variability on QDs FWHM. It is seen that both the maximum and minimum attainable CAF have their optimal values within the variation of QDs FWHM. The minimum CAF reaches its optimal value of 0.241 at 2700 K with QDs FWHM = 40 nm, and the maximum CAF reaches its optimal value of 0.995 at 6500 K with QDs FWHM = 30 nm. As a consequence, the circadian variability has its maximized value of 4.01 at QDs FWHM = 40 nm. It is worth noting that a broad QDs FWHM will result in a significant decrease of circadian variability. For instance, at QDs FWHM = 100 nm, which is the typical value of red phosphor, the circadian variability drops to 2.94. Therefore, with narrow FWHM of 30 nm ~ 50 nm, red-emissive QDs are suitable for the variability of circadian actions of WLEDs.

3.2. Experimental validation

Figure 6 shows the high-resolution transmission electron microscope (HRTEM) and scanning electron microscope (SEM) images and spectra of the as-prepared QDs. From figures 6(a)–(b), the core–shell QDs average size is measured as 6.4 nm with uniform size distribution and clear lattice fringes. Figure 6(c) demonstrate the SEM images of the as-fabricated QDs-LMS, whose diameters range from 20–40 μm.

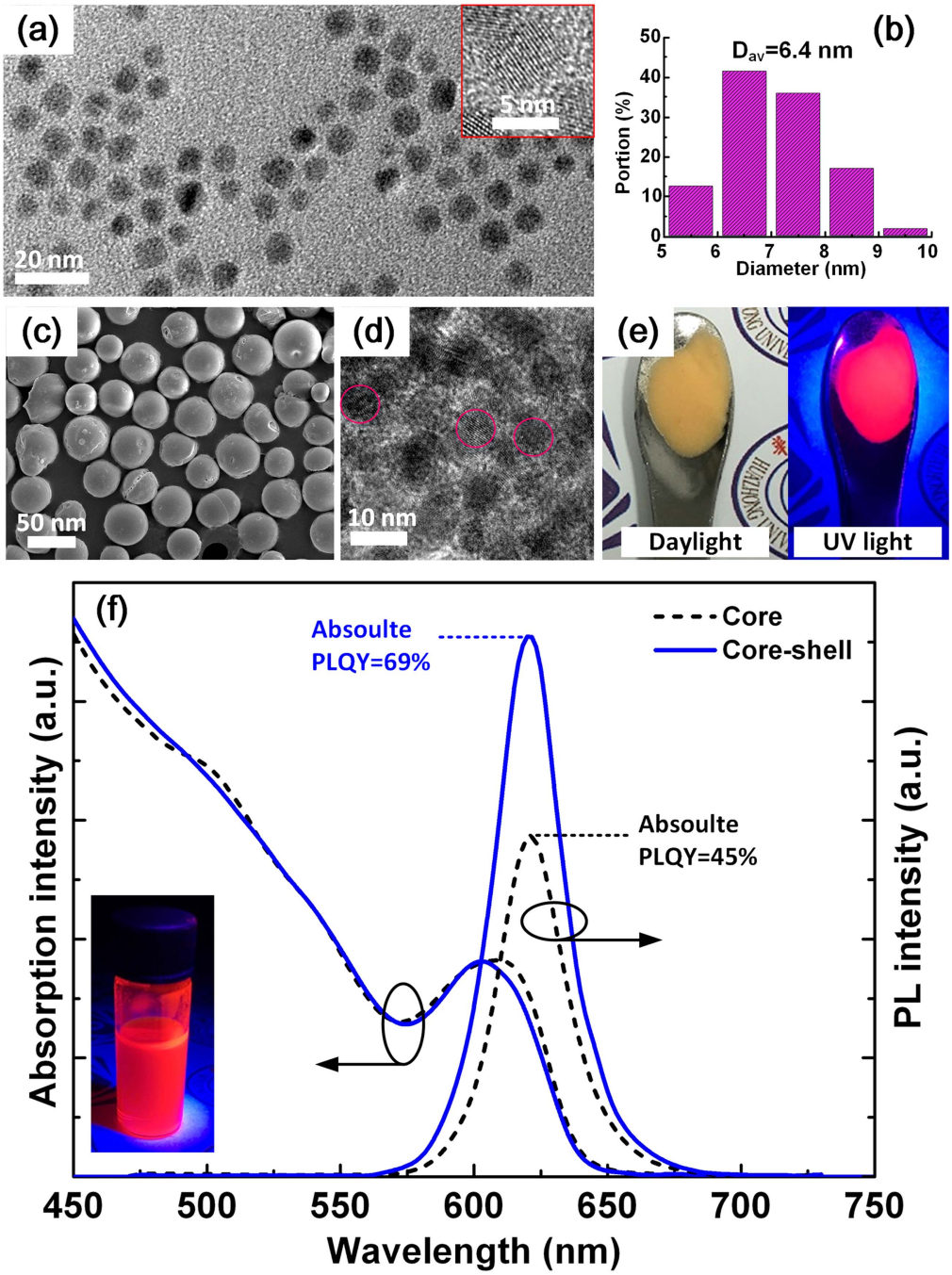

Figure 6. (a) HRTEM images and (b) size distribution of the as-prepared CdSe/ZnS QDs. (c) SEM image and (d) HRTEM images of the as-fabricated QDs-LMS. (e) Photographs of the QDs-LMS under daylight and UV light, respectively. (f) Normalized absorption and PL spectra of the core and core–shell QDs.

Figure 6(d) shows the HRTEM image of the QDs-LMS, which confirms the incorporation of QDs into the mesoporous. Benefitting from the TOP-assisted SILAR method, which removes the surface lattice imperfections by surface ion re-dissolution and lattice rearrangement during the whole ZnS shell formation process, the absolute photoluminescence quantum yield (PLQY) was enhanced efficiently from 45% (core) to 69% (core–shell), as depicted in figure 6(f). The absolute PLQY decreases from 69% in solution to 64% in mesoporous silica. Therefore, the PLQY of QDs still remains at a large extent of 92.8% after being incorporated into mesoporous silica. It is worth noting that the absorption spectrum of core–shell QDs varies little from the core QDs, which is mainly attributed to the relatively thin shell coating (~0.3 nm).

Based on above optimization results, we fabricated a series of QDs-WLEDs samples with different CCTs to validate their circadian variability. The samples with low and high CCTs were tuned to achieve a minimum and maximum CAF, respectively, to obtain a wide circadian variability. Meanwhile,

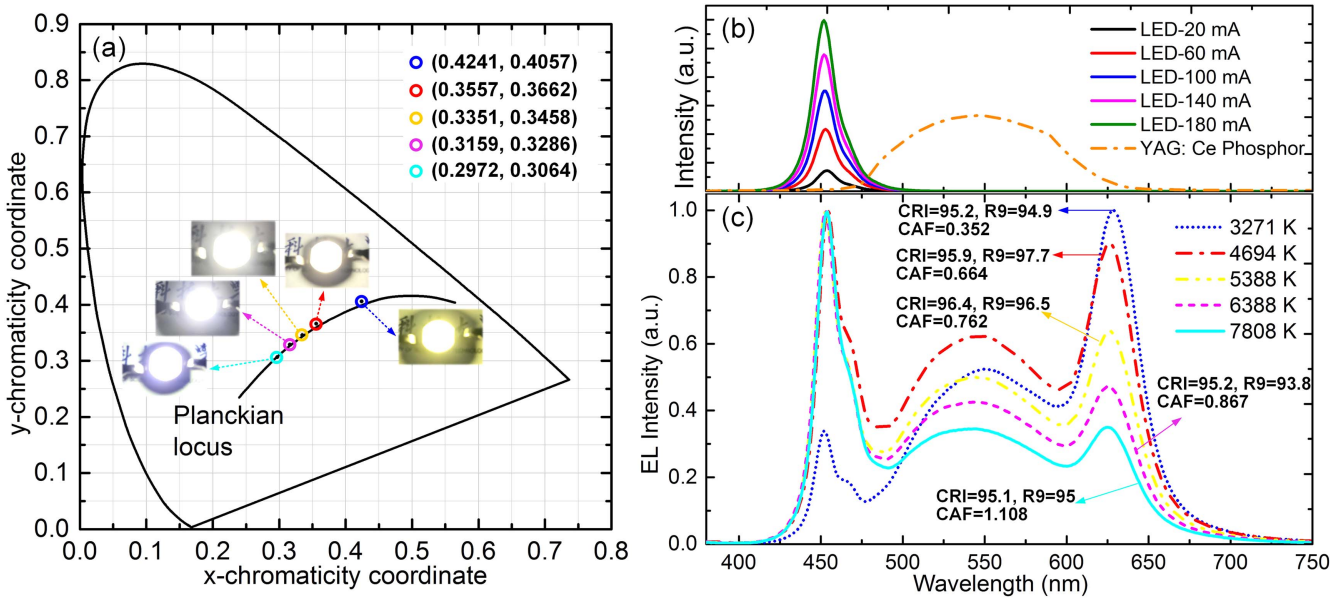

Figure 7. (a) CIE diagram and color coordinates of those as-fabricated QDs-WLEDs. Insets show their photographs illuminated at 20 mA. (b) EL spectra of bare LED chip under varying driving current, and the PL spectrum of YAG: Ce phosphor. (c) EL spectra of those QDs-WLEDs at 3271 K, 4694 K, 5388 K, 6388 K, and 7808 K.

all the samples were restricted by CRI $>$ 95 and R9 $>$ 90, which indicates the color rendering ability towards deep red.

Figure 7 shows the color coordinates and spectra of those as-fabricated QDs-WLEDs with CCT of 3271 K, 4694 K, 5388 K, 6388 K, and 7808 K. At CCT of 3271 K, the CAF value is calculated as 0.352 (about 97% of the CAF value of a 2700 K incandescent lamp), which is suitable for night lighting. With the increase of CCT, the blue part of SPD increases, leading to the rise of minimum attainable CAF. The CAF value increased to 1.108 at CCT of 7808 K, which is about 110% of the CAF value of the CIE standard daylight illuminant D_{65}. Therefore, this light source can be used for office workplace illumination. The experimental circadian variability was calculated as 3.15, with a high CRI of Ra $>$ 95 and R9 $>$ 93.

According to our results, excellent LE reaching up to 142.5 lm W^{-1} with Ra = 90 and R9 = 95 at 20 mA was achieved, which is a new record of QDs-WLEDs from previous literature [17]. This is mainly attributed to the large number of surviving high-efficiency QDs in LMS after the solvent evaporation method and high-temperature curing. Secondly, the lifetime of the whole device is decided by the lifetime of the QDs layer. We also evaluated the luminescence decay of QDs-WLEDs under a severe circumstance with high temperature (85 °C) and high relative humidity (85%) for about 200 h. It shows that the QDs-WLEDs preserve 86% of optical power after an accelerated ageing process, while the red-phosphor-based WLEDs preserve 92.4% of optical power.

Moreover, the stability under versus current injection has been tested as well. When driving current was increased from 20–200 mA, the CCT increased from 5203–5430 K, LE decreased from 142.5 lm W^{-1} to 116 lm W^{-1}, and CRI varied from 90–86. Therefore, these lifetime and stability performances are close to state-of-the-art WLEDs using phosphor. In addition, QDs-LMS is fully compatible with the current LED packaging process and can be used as phosphors for direct on-chip applications, indicating that the processing reproducibility of QDs-WLEDs is catching up with that of commercial LEDs.

4. Conclusion

In conclusion, we proposed an approach to maximized circadian variability based on QDs-WLEDs. The limiting circadian variability was found to decrease when reinforcing the constraints on the CRI. For constant CCTs, the CAF of the QDs-WLEDs can be tuned above and below that of the corresponding black-body radiators and common pc-LEDs. Too narrow or too broad QDs FWHM will limit the variability of CAF, and a QDs spectrum component with FWHM of 20 nm $\sim$ 40 nm is suitable for wide circadian variability. At CRI $>$ 90, the maximum CAF variability can be tuned by 3.83 times (from 0.251 at 2700 K to 0.961 at 6500 K). Our approach could reduce the number of tunable channels, and could achieve wider CAF variability than previous solutions. Based on the optimization results, we fabricated several QDs-WLEDs samples with different CCTs. The as-prepared QDs-WLEDs achieved circadian variability of 3.15 times (from 0.352 at 3721 K to 1.108 at 7808 K) with Ra $>$ 95 and R9 $>$ 93. The established limits of the CAF variability of QDs-WLEDs can be used as guidelines for the development of light sources with dynamically modulated circadian efficacy.

Acknowledgments

This work is supported by the National Natural Science Foundation of China (NFSC) (51625601, 61604135 and 51402148) and the Guangdong Innovation Project (2014A010105005, 2014TQ01C494). The authors would like to thank Tianjin Zhonghuan Quantum Tech Co. Ltd for technical support with the fabrication of WLEDs.

References

[1] Pimputkar S, Speck J S, DenBaars S P and Nakamura S 2009 Prospects for LED lighting *Nat. Photon.* **3** 180–2
[2] Luo X, Hu R, Liu S and Wang K 2016 Heat and fluid flow in high-power LED packaging and applications *Prog. Energ. Combust. Sci.* **56** 1–32
[3] Jang H S and Jeon D Y 2007 White light emission from blue and near ultraviolet light-emitting diodes precoated with Sr_3SiO_5: Ce^{3+}, Li^{+} phosphor *Opt. Lett.* **32** 3444–6
[4] Ma Y, Hu R, Yu X, Shu W and Luo X 2017 A modified bidirectional thermal resistance model for junction and phosphor temperature estimation in phosphor-converted light-emitting diodes *Int. J. Heat Mass Tran.* **106** 1–6
[5] Jang H S, Im W B, Lee D C, Yeon D Y and Kim S S 2007 Enhancement of red spectral emission intensity of $Y_3Al_5O_{12}$:Ce^{3+} phosphor via Pr co-doping and Tb substitution for the application to white LEDs *J. Lumin.* **126** 371–7
[6] Pauley S M 2004 Lighting for the human circadian clock: recent research indicates that lighting has become a public health issue *Med. Hypotheses* **63** 588–96
[7] Cajochen C, Munch M, Kobialka S, Krauchi K, Steiner R, Oelhafen P, Orgul S and Wirz-Justice A 2005 High sensitivity of human melatonin, alertness, thermoregulation, and heart rate to short wavelength light *J. Clin. Endocr. Metab.* **90** 1311–6
[8] Zeitzer J M, Dijk D J, Kronauer R E, Brown E N and Czeisler C A 2000 Sensitivity of the human circadian pacemaker to nocturnal light: melatonin phase resetting and suppression *J. Physiol.* **526** 695–702
[9] Navara K J and Nelson R J 2007 The dark side of light at night: physiological, epidemiological, and ecological consequences *J. Pineal. Res.* **43** 215–24
[10] Blask D E, Hill S M, Dauchy R T, Xiang S, Yuan L, Duplessis T, Mao L, Dauchy E and Sauer L A 2011 Circadian regulation of molecular, dietary, and metabolic signaling mechanisms of human breast cancer growth by the nocturnal melatonin signal and the consequences of its disruption by light at night *J. Pineal. Res.* **51** 259–69
[11] Falchi F, Cinzano P, Elvidge C D, Keith D M and Haim A 2011 Limiting the impact of light pollution on human health, environment and stellar visibility *J. Environ. Manage.* **92** 2714–22
[12] Hoffmann G, Gufler V, Griesmacher A, Bartenbach C, Canazei M, Staggl S and Schobersberger W 2008 Effects of variable lighting intensities and colour temperatures on sulphatoxymelatonin and subjective mood in an experimental office workplace *Appl. Ergon.* **39** 719–28
[13] Figueiro M G 2008 A proposed 24 h lighting scheme for older adults *Light. Res. Technol.* **40** 153–60
[14] de Kort Y A W and Smolders K C H J 2010 Effects of dynamic lighting on office workers: first results of a field study with monthly alternating settings *Light. Res. Technol.* **42** 345–60
[15] Xiao X, Tang H, Zhang T, Chen W, Wu D, Wang R and Wang K 2016 Improving the modulation bandwidth of LED by CdSe/ZnS quantum dots for visible light communication *Opt. Express* **24** 21577–86
[16] Xie B, Hu R and Luo X 2016 Quantum dots-converted light-emitting diodes packaging for lighting and display: status and perspectives *J. Electron. Packag.* **138** 020803
[17] Chen W *et al* 2016 High efficiency and color rendering quantum dots white light emitting diodes optimized by luminescent microspheres incorporating *Nanophotonics* **5** 565–72
[18] Azkauskas A, Vaicekauskas R and Vitta P 2012 Optimization of solid-state lamps for photobiologically friendly mesopic lighting *Appl. Opt.* **51** 8423–32
[19] Deb K 2000 An efficient constraint handling method for genetic algorithms *Comput. Method. Appl.* M **186** 311–38
[20] Long Q and Wu C 2014 A hybrid method combining genetic algorithm and Hooke–Jeeves method for constrained global optimization *J. Ind. Manag. Optim.* **10** 1279–96
[21] Hao J, Zhou J and Zhang C 2013 A tri-n-octylphosphine-assisted successive ionic layer adsorption and reaction method to synthesize multilayered core–shell CdSe-ZnS quantum dots with extremely high quantum yield *Chem. Comm.* **49** 6346–8
[22] Song W S and Yang H 2012 Fabrication of white light-emitting diodes based on solvothermally synthesized copper indium sulfide quantum dots as color converters *Appl. Phys. Lett.* **100** 183104
[23] Song W S and Yang H 2012 Efficient white-light-emitting diodes fabricated from highly fluorescent copper indium sulfide core/shell quantum dots *Chem. Mater.* **24** 1961–7
[24] Song W S, Kim J H, Lee J H, Lee H S, Do Y and Yang H 2012 Synthesis of color-tunable Cu-In-Ga-S solid solution quantum dots with high quantum yields for application to white light-emitting diodes *J. Mater. Chem.* **22** 21901–8
[25] Jang E P, Song W S, Lee K H and Yang H 2013 Preparation of a photo-degradation-resistant quantum dot-polymer composite plate for use in the fabrication of a high-stability white-light-emitting diode *Nanotechnology* **24** 045607
[26] Zukauskas A and Vaicekauskas R 2015 Tunability of the circadian action of tetrachromatic solid-state light sources *Appl. Phys. Lett.* **106** 041107
[27] Dai Q, Shan Q, Lam H, Hao L, Lin Y and Cui Z 2016 Circadian-effect engineering of solid-state lighting spectra for beneficial and tunable lighting *Opt. Express* **24** 20049–59
[28] Yang X, Zhao D, Leck K S, Tan S T, Tang Y X, Zhao J, Demir H V and Sun X W 2012 Full visible range covering InP/ZnS nanocrystals with high photometric performance and their application to white quantum dot light-emitting diodes *Adv. Mater.* **24** 4180–5
[29] Chen O *et al* 2013 Compact high-quality CdSe-CdS core–shell nanocrystals with narrow emission linewidths and suppressed blinking *Nat. Mater.* **12** 445–51
[30] Altintas Y, Talpur M Y, Unlu M and Mutlugun E 2016 Highly efficient Cd-free alloyed core/shell quantum dots with optimized precursor concentrations *J. Phys. Chem.* C **120** 7885–92